Z. Kristallogr. Suppl. **26** (2007) 17-26

Nanostructure studied using the atomic pair distribution function

S. J. L. Billinge*

Department of Physics and Astronomy, Michigan State University, East Lansing, MI 48824
* billinge@pa.msu.edu

Keywords: pair distribution function, structure, nanoparticles, nanoporous materials, nanostructured bulk materials

Abstract. Studying the atomic structure of nanostructured materials presents a special challenge because our extensive crystallographic toolbox begins to lose its power on the nanoscale. The presumption of periodicity is a poor approximation when structural correlation lengths are limited to a few tens of nanometres or less and alternative approaches are needed. Here we give an overview of recent results where the use of the atomic pair distribution function analysis of x-ray and neutron powder diffraction has yielded useful insights in different classes of nanostructure problem.

Introduction

Crystallography has been the mainstay of structure studies for almost 100 years since it was first developed in the pioneering work of Max von Laue [1] and the Braggs [2] in the second decade of the 20th century. The basic presumption is one of crystallinity: that the structure is made up of an infinite periodic array of identical units. As a result the diffraction occurs in sharp Bragg-peaks that are periodically arrayed in reciprocal space. Powerful algorithms exist to reconstruct the 3D arrangement of atoms that gives rise to a particular pattern of Bragg peaks allowing structures to be solved in many, if not most, cases. This is true even in the more severely limited case of a powder diffraction pattern where directional information is explicitly lost [3]. In favourable circumstances it can be reconstructed and a 3D structure solved from 1D data.

Real crystals do not conform to the ideal of perfectly reproduced identical units that extend to infinity. Defects and lattice vibrations destroy the identicality, and crystals are not infinitely large. The methods of crystallography are robust against these imperfections making them of enormous practical value. However, as the crystallite size approaches the nanometer scale, the presumption of crystallinity becomes an increasingly poor starting point. Structures with correlations that extend only on the nanometer length-scale scatter x-rays and neutrons in broad diffuse patterns of intensity and not into sharp Bragg peaks.

Diffraction is still highly useful in studying short-range atomic order in materials and has been extensively used to study amorphous materials and liquids [4]. In this case the structural coherence length is limited to around 1 nm and only a statistical description of the structure is possible. Understanding the structure of glasses and the glass transition remains one of the outstanding challenges in physics.

Nanostructured materials lie between the extremes of amorphous and crystalline materials. They include discrete nanoparticles, nanoporous materials with, or without, species intercalated in the pores, and nanostructured bulk crystals (NBC's) that have structural fluctuations on the nanoscale superimposed on an average crystal structure. Obtaining detailed structural information in these cases is of great, and increasing, importance with the growth of nanotechnology. Materials that are nanostructured have emergent properties that are qualitatively different to those of the equivalent macroscopic materials. There is a drive to design and engineer this nanoscale structure to obtain specific properties. Clearly, a prerequisite is to characterize the atomic structure on this scale. However, as we discussed above, this is precisely the domain where the crystallographic methods lose their power. This we refer to as the "nanostructure problem". It is more than an unfortunate coincidence: it is one of the emergent properties of the nanoscale materials. Non-crystallographic methods are required to solve these nanostructure problems.

Here we give an overview on progress using the atomic pair distribution function (PDF) method for studying nanostructured materials, focussing on developments in the Billinge group.

The atomic pair distribution function (PDF) method

The PDF method has been described in detail in a number of other sources. Brief and accessible introductions are given in [5] and [6]. The method is described in much more detail in Egami and Billinge [7]. These descriptions of the method are particularly relevant to the application of the PDF to disorder in crystals and to nanostructured materials in general.

The atomic PDF, *G(r)*, is defined as

$$G(r) = \frac{1}{r}\sum_{\nu}\sum_{\mu}\frac{f(0)_{\nu} f(0)_{\mu}}{\langle f(0)\rangle^2}\delta(r - r_{\nu\mu}) - 4\pi r\rho_0 .^{1} \qquad (1)$$

where ρ_o is the average atomic number density, δ is the Dirac delta function, $r_{\nu\mu}$ is the distance separating the νth and μth atoms and the sums are over all the atoms in the sample. Here the *f(0)*'s are the atomic form factors evaluated at Q=0 that are, to a good approximation, given by the number of electrons on the atom, Z. In the case of neutron diffraction the *f(0)*'s should be replaced by neutron scattering lengths, b_{ν}. The angle brackets in the denomi-

[1] There is a lack of standardization on nomenclature that has arisen historically so different groups use different letters for the various functions. This has been explored in detail by Keen [8]. In any given paper on the PDF method, readers should beware of this and make sure they understand the definition of the various functions being quoted.

nator indicate the average value. This shows how *G(r)* can be directly calculated from the atomic structure. It is made up of a series of delta functions that occur at the distances *r* such that two atoms are separated by that distance. The total pair distribution function is built up by summing over all atom-pairs in the solid. This is shown schematically in figure 1.

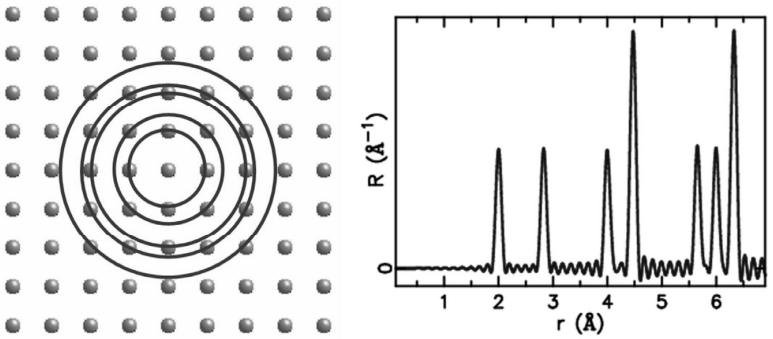

Figure 1. Schematic of how the total pair distribution function is built up by finding atoms at a distance, r, from an atom at the origin. Circles indicate distances where neighbours to the central atom exist and these correspond to peaks in the radial distribution function shown on the right. The number of atoms on the circle is the multiplicity (scale) of that peak. The scattering power of each atom in the pair also contributes to this scale, as per equation (1). The total pair distribution function is obtained by repeating this process systematically by placing each atom at the origin.

Thus, given a structural model we can calculate *G(r)* straightforwardly. *G(r)* is also an experimentally accessible function. It is related to the measured x-ray or neutron powder diffraction pattern through a Fourier transform,

$$G(r) = \frac{2}{\pi}\int_{Q_{\min}}^{Q_{\max}} Q[S(Q)-1]\sin(Qr)dQ\,. \qquad (2)$$

Here Q is the magnitude of the scattering vector or momentum transfer. For elastic scattering, $Q=4\pi\sin\theta/\lambda$, where 2θ is the diffraction angle and λ the wavelength of the x-rays or neutrons. Q_{min} and Q_{max} define the experimentally determined range over which data were collected. Q_{max} is often limited by the statistics on the data with better statistics allowing for a higher Q_{max}. A wider Q-range is better. In particular, it is important to push Q_{max} as high as possible to increase real-space resolution and decrease spurious termination ripples from the Fourier transform. *S(Q)* is the properly normalized powder diffraction pattern from the sample. It is formally defined as

$$S(Q) = \frac{I^{coh}(Q) - \sum c_i |f_i(Q)|^2}{\left|\sum c_i f_i(Q)\right|^2} + 1\,. \qquad (3)$$

Here $I^{coh}(Q)$ is the coherent scattering intensity, which is the powder pattern that has been corrected for experimental effects, such as background scattering, detector dead-time and

efficiency, sample dependent effects, such as Compton and multiple scattering, and normalized for incident flux. The sums are over all atomic species in the material where the concentration of species *i* is c_i. The vertical lines indicate taking the modulus squared , i.e., the product of the real and imaginary parts. This is relevant close to an absorption edge where *f* has an imaginary anomalous correction term. This equation shows that *S(Q)*, and therefore *G(r)* can be straightforwardly determined from a powder diffraction measurement. Also of interest is the fact that the definition of *S(Q)* has in the denominator the square of the atomic form factor. This form factor becomes small for x-rays at high *Q*-values. By dividing the measured intensity by this value there is a relative enhancement in the high-*Q* scattering. This region of the data often contains valuable information that is ignored in conventional analyses of powder data. The effect of this is illustrated for a $Mo_6S_xI_{10-x}$ nanowire and crystalline MoS_2 in figure 2. A number of programs are available for carrying out the data corrections to get *G(r)* from raw data. The software repository ccp14 [9] is a good resource. A user friendly program with some time-saving features and built in plotting that was written by the Billinge-group is PDFgetX2 that is available from the totalscattering website [10].

As mentioned above, the PDF, often referred to as radial distribution function or RDF analysis, has a long and rich history, going back to the pioneering work of Debye [11], Warren [12] and others, as applied to the study of structure in glasses, liquids and amorphous

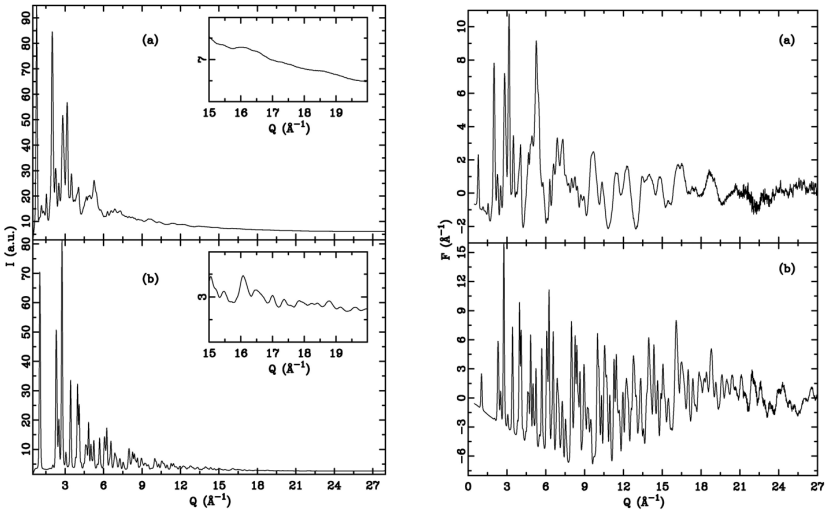

Figure 2. raw intensities and reduced structure functions, F(Q)=Q[S(Q)-1], for representative samples. Top panels are data from $Mo_6S_xI_{10-x}$ nanowires and below are from a MoS_2 crystalline analogue. The data are plotted over the same Q-range in the left and right panels. Notice the extensive diffuse scattering at high-Q that emerges in the properly normalized data [16].

materials. Alternative descriptions of the method as applied in these earlier studies can be found in a number of books, notably, those by Warren [13] and Klug and Alexander [14]. Modern applications of the method, both in the disordered- and nanostructured materials

domains, benefit enormously from the use of synchrotron x-ray sources and spallation neutron sources which provide high fluxes of high energy x-rays and neutrons, respectively. Another important development that is revolutionizing the quantitative information that can be obtained from this technique is the availability of fast (and inexpensive) computers. As a result, coupled with the growing need to characterize structure on the nanoscale, the PDF method has greater relevance than every before in structural studies of nanostructured materials.

Quantitative modelling of the data is a frontier area where great strides have been taken in the past few years. Beyond fitting Gaussian peaks to individual features in the PDF, long a staple in the disordered materials regime and still a powerful and intuitive approach, full-profile fitting of *S(Q)* or *G(r)* has been developed more recently and is proving very effective. Approaches based on rather unconstrained Monte Carlo simulated annealing, the reverse Monte Carlo method, are most widely used for amorphous and liquid materials [17,18]. For nanostructured materials two other approaches are more widely used. The first is the real-space equivalent of Rietveld refinement where the structure is represented by a rather small unit cell, though typically larger than the crystalline one since we are interested in disorder in the crystal. The programs used there are called PDFfit [19] which has now been significantly improved and released with a graphical user interface (gui) [20]. These are available from the totalscattering web-site [10]. The other approach uses ideas from both the structure refinement and Monte Carlo worlds. It uses a Monte Carlo algorithm but basically carries out structure refinement by fitting Bragg intensities at the same time as total scattering data in real and/or reciprocal space [21]. A number of other novel modelling approaches are emerging, including structure solution for nanoparticles [22], but it is beyond the scope of this overview to discuss them.

Nanoparticles and nanowires

The archetypal nanomaterials are discrete nanoparticles. These began to be explicitly produced beginning in the late 1980's [23]. Most early structural studies, with some notable exceptions [24], on these materials was qualitative or semi-quantitative in nature and relied on studying conventional powder diffraction patterns, TEM images and the like. EXAFS has also been used [25]. More recently, the power of PDF analysis has been directed in this direction with some success [26-30]. Quantitative structural information can be extracted about the structure of the crystalline core, the size, and to a lesser extent the shape of the nanoparticle, the existence or otherwise of surface reconstructions and the presence of internal strains [31]. The PDF technique should become much more ubiquitous as a sample characterization tool for nanoparticles in the future.

Structure solution of nanoparticles is also a big issue when the initial structure is not known. There is a single demonstration of real *ab initio* structure solution for a model system [22]. However, it is possible to determine nanoparticle structure by a trial and error method where good structure candidates are known, for example, crystalline analogues. There are a number of good demonstrations of this, including hydrated vanadium xerogel materials [32] and nanocrystalline intercalated MoS_2 [33] among others. We recently also demonstrated the

structure of the technologically interesting $Mo_6S_xI_{10-x}$ nanowires [34] using PDF modelling [16]. The raw and normalized data-sets are shown in figure 1. In figure 3 we show the resulting PDF with the PDF calculated from the successful structural model superimposed. The resulting structural model for the nanowires is illustrated in the right panel of the figure.

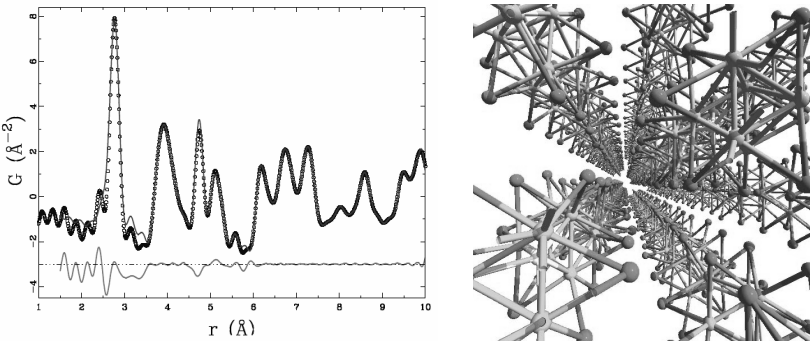

Figure 3. (left) Pair distribution functions from the $Mo_6S_xI_{10-x}$ nanowires. The symbols are the data and the line is the calculated PDF from the successful structural model. The curve offset below is the difference between the measured and calculated PDFs. (right) representation of the resulting structural model [16].

Nanostructured bulk crystals

A large and growing class of nanostructured materials are bulk crystals that, nonetheless, have a local structure that is significantly different from that inferred from the crystal structure. The crystallographic structure is the periodically averaged version of the structure. Local domains of chemical or displacive order that are not periodic are lost in the crystal structure determination. The PDF, and total scattering in general, is proving enormously useful for studying these structural fluctuations. We refer to materials where this is an issue as nanostructured bulk crystals (NBC's). They can be studied directly by analyzing diffuse scattering in single crystal samples [35,36].Although this approach yields more information than a powder measurement, difficulties in measuring the data and carrying out quantitative modelling has limited the impact. Local structure in NBCs can also be analyzed from total scattering measurements of powders and there are a number of successful studies in this arena. Examples include the direct observation of polaron formation at the metal-insulator transition in colossal magnetoresistant manganites [37], studies of the phase transitions in silica [38] and fluoride phases [39] and discommensurations in incommensurate charge density wave materials [40] among many others.

An interesting twist on these studies is the use of *r*-dependent refinements to extract different structural information on different length-scales. A nice demonstration of this is in the orbital order-disorder phase transition of the undoped endmember of the cubic manganites, $LaMnO_3$ [41]. Short range orbital order of the Jahn-Teller distorted MnO_6 octahedra persists in the high temperature phase in this material [42]. Crystallographically, this phase is pseudo-cubic with virtually no Jahn Teller distortion surviving in the structure model. The

PDF allowed information to be extracted about the short-range ordering of the JT distorted orbitals by refining the PDF over different ranges of *r* [43]. This is illustrated in figure 4.

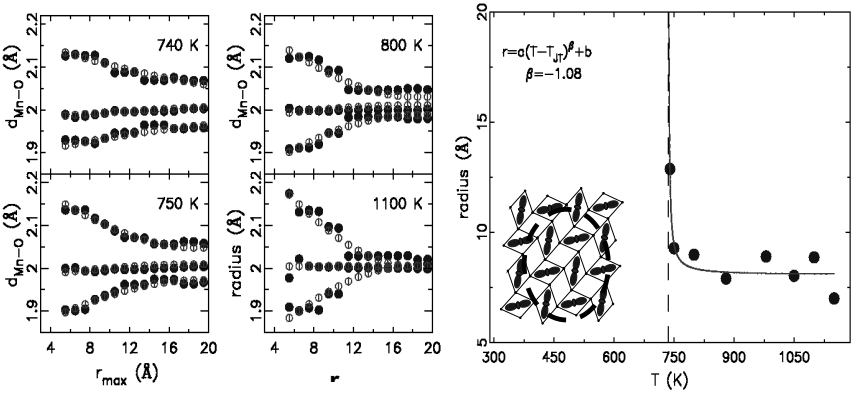

Figure 4. Left panels (filled circles) long and short Mn-O bonds in the JT distorted MnO_6 octahedra as refined from the PDF data where the refinements were carried out over different ranges of the PDF. Refinements confined to low-r show the JT distortions. For the higher temperature data-sets in the pseudo-cubic phase, the higher r-range refinements indicate no JT distortion in agreement with the crystallographic structure. The open circles indicate the expected crossover assuming spherical regions of local order. From this a semi-quantitative estimate of the correlation length of the orbital ordering was extracted and is plotted in the right panel. The inset in this panel indicates the nature of the local orbital ordering in the high temperature phases [43].

Nanoscale structures are now being utilized and engineered into materials to improve properties such as thermoelectricity [44,45] and fast ion conductivity [46] among other properties.

Nanoporous materials

Nanoporous materials, more conventionally called, mesoporous materials, have pore structures that are nanoscale in dimension. Structural problems in these materials involve characterizing the porous matrix, but of increasing importance is the need to know the local structure of species intercalated into these pores. Again the PDF can play a valuable role here and there are a number of excellent examples where intercalants were characterized in this way. The charge state of Cs in zeolite ITQ-4 was shown to be 1+ identifying the composite material as an inorganic electride [47]. The local bonding environment of mercury was elucidated in a functionalized silica host that has potential use as a mercury getter in environmental remediation [48]. More recently we were able to carry out a multi-phase determination of the structure of reaction products in an intercalated system of sodium in silica gel, a non pyrophoric reducing agent that also has great industrial potential [49]. Again, there is a good match between the growing need to characterize materials of this sort, and the growing power of PDF methods to do it.

Conclusion

The application of PDF methods is growing in number and importance. There are a number of reasons for this. First and foremost is the complex, nanostructured, nature of novel functional materials that are being discovered and developed these days. Conventional diffraction methods tell only part of the story, or no story at all, in these materials and there is great added value in using PDF methods. Second, the experimental methods and tools are advancing to the point where these experiments are straightforward and quick. A significant recent breakthrough in this department was the development of a rapid acquisition mode, RAPDF, for x-ray PDFs at synchrotron sources [50]. There is now a dedicated beamline at the advanced photon source (11ID-B) for these measurements with more planned at NSLS and ESRF. These experiments are also possible at other high energy beamlines at the synchrotron facilites, greatly expanding the number of experiments, and experimenters, that can use PDF methods. It is also only a matter of time before laboratory instruments optimized for these measurements are produced commercially. Finally, the data modelling and extraction of structural information from the data is increasing in sophistication and ease of use [20], again increasing both the scope and breadth of science possible with the method.

References

1. Friedrich, W., Knipping, P., & Laue, M., 1913, *Ann. Phys.-Berlin*, **41**, 971--988, reprinted from *Sitzungsber. K. Bayer. Akad. Wiss.* pp. 303-322, (1912).
2. Bragg, W. H., 1914, *Science*, **40**, 795—802.
3. David, W. I. F., Shankland, K., McCusker, L. B., & Baerlocher, C. (eds), 2002, Structure Determination from Powder Diffraction Data (Oxford: Oxford University Press).
4. Wright, A. C., 1998, *Glass. Phys. Chem.,* **24**, 148—179.
5. Billinge, S. J. L. & Kanatzidis, M. G., 2004, *Chem. Commun*., 749—760.
6. Proffen T., Billinge, S. J. L., Egami, T. & Louca, D., 2003, *Z. Kristallogr*., **218** 132—143.
7. Egami, T. & Billinge, S. J. L., 2003, Underneath the Bragg peaks: structural analysis of complex materials (Oxford, England: Pergamon Press, Elsevier).
8. Keen, D. A., 2001. *J. Appl. Crystallogr*., **34**, 172—177.
9. http://www.ccp14.ac.uk
10. http://www.totalscattering.org
11. Debye, P. & Menke, H., 1930, *Physik. Z*., **31,**, 797—8.
12. Warren, B. E., Krutter, H. & Morningstar, O., 1936, *J. Am. Ceram. Soc.,* **19,** 202—6.
13. Tarasov, L. P. & Warren, B. E., 1936, *J. Chem. Phys.,* **4,** 236—8.
14. Warren, B. E., 1990, X-ray diffraction (New York: Dover).

15. Klug, H. P. & Alexander, L. E., 1974, X-ray diffraction procedures for polycrystalline and amorphous materials 2nd ed (New York: Wiley).
16. Paglia, G., Bozin, E. S., Vengust, D., Mihailovic, D. & Billinge, S. J. L., 2006, *Chem. Mater.,* **18,** 100—106.
17. McGreevy, R. L. & Pusztai, L., 1988, *Mol. Simul.,* **1,** 359—367.
18. McGreevy, R. L., 2001, *J. Phys.: Condens. Mat.,* **13,** R877--R913.
19. Proffen, T. & Billinge, S. J. L., 1999, *J. Appl. Crystallogr.,* **32,** 572—575.
20. Farrow, C. L., Juhas, P., Liu, J. W., Bryndin, D., Bloch, J., Proffen, T., & Billinge S. J. L., 2006, *J. Phys: Condens. Matter,* To be published.
21. Tucker, M. G., Dove, M. T. & Keen, D. A., 2001, *J. Appl. Crystallogr.,* **34,** 630—638.
22. Juhas, P., Cherba, D. M., Duxbury, P. M., Punch, W. F. & Billinge, S. J. L., 2006, *Nature,* **440,** 655—658.
23. Steigerwald, M. L. & Brus, L. E., 1989, *Annu. Rev. of Mater. Sci.,* **19,** 471—495.
24. Bawendi, M. G., Kortan, A. R., Steigerwald, M. L. & Brus, L. E., 1989, *J. Chem. Phys*., **91,** 7282—7290.
25. Marcus, M. A., Flood, W., Stiegerwald, M., Brus, L. & Bawendi, M., 1991, *J. Phys. Chem*., **95** 1572—1576.
26. Gilbert, B., Huang, F., Zhang, H., Waychunas, G. A. & Banfield, J. F., 2004, *Science,* **305,** 651—654.
27. Neder, R. B. & Korsunskiy, V. I., 2005, *J. Phys.: Condens. Mat.,* **17,** S125--S134.
28. Page, K., Proffen, T., Terrones, H., Terrones, M., Lee, L., Yang, Y., Stemmer, S. Seshadri, R. & Cheetham, A. K., 2004, *Chem. Phys. Lett*., **393,** 385—388.
29. Petkov, V., Gateshki, M., Choi, J., Gillan, E. G. & Ren, Y., 2005, *J. Mater. Chem.,* **15,** 4654.
30. Gateshki, M., Petkov, V., Williams, G., Pradhan, S. K. & Ren, Y., 2005, *Phys. Rev. B,* **71,** 224107.
31. Masadeh, A. S., Bozin, E. S., Farrow, C. L., Paglia, G., Juhas, P., Karkamkar, A., Kanatzidis, M. G. & Billinge, S. J. L., 2007, *Phys. Rev. B,* Submitted.
32. Petkov, V., Trikalitis, P. N., Božin, E. S., Billinge, S. J. L., Vogt T. and Kanatzidis, M. G., 2002, *J. Am. Chem. Soc.* **124**, 10157.
33. Petkov, V., Billinge, S. J. L., Larson, P., Mahanti, S. D., Vogt, T., Rangan, K. K. and Kanatzidis, M. G., 2002, *Phys. Rev. B,* **65**, 092105.
34. Remskar, M., Mrzel, A., Skraba, Z., Jesih, A., Ceh, M., Demsar, J., Stadelmann, P., Levy, F. & Mihailovic, D., 2001, *Science,* **292,** 479—481.
35. Welberry, T. R., 2004, Diffuse x-ray scattering & models of disorder (Oxford: Oxford University Press).
36. Campbell, B., Argyriou, D., Mitchell, J., Osborn, R., Ouladdiaf, B. & Ling, C., 2004, *Phys. Rev. B,* **69,** 104403.

37. Billinge, S. J. L., DiFrancesco, R. G., Kwei, G. H., Neumeier, J. J. & Thompson, J. D., 1996, *Phys. Rev. Lett*., **77,** 715—718.
38. Tucker, M. G., Squires, M. P., Dove, M. T. & Keen, D. A., 2001, *J. Phys.: Condens. Mat.,* **13,** 403—423.
39. Chupas, P. J., Chaudhuri, S., Hanson, J. C., Qiu, X., Lee, P. L., Shastri, S. D., Billinge, S. J. L. & Grey, C. P., 2004, *J. Am. Chem. Soc*., **126,** 4756—4757.
40. Kim, H. J., Malliakas, C. D., Tomic, A., Tessmer, S. H., Kanatzidis, M. G. & Billinge, S. J. L., 2006, *Phys. Rev. Lett*., **96,** 226401.
41. Chatterji, T., Fauth, F., Ouladdiaf, B., Mandal, P. & Ghosh, B., 2003, *Phys. Rev. B,* **68,** 052406 (pages. 4).
42. Sanchez, M. C., Subias, G., Garcia, J. & Blasco, J., 2003, *Phys. Rev. Lett.,* **90,** 045503 (pages. 4).
43. Qiu, X., Proffen, Th., Mitchell, J. F. & Billinge, S. J. L., 2005, *Phys. Rev. Lett*., **94,** 177203.
44. Lin, H., Bozin, E S., Billinge, S. J. L., Quarez, E. & Kanatzidis, M. G., 2005, *Phys. Rev. B,* **72,** 174113.
45. Kim, H. J., Bozin, E. S., Haile, S. M., Snyder, G. J. & Billinge, S. J. L., 2007, *Phys. Rev. B,* To be published.
46. Malavasi, L., Billinge, S. J. L., Kim, H. J., Proffen, T., Tealdi, C. & Flor, G., 2007, *J. Am. Chem. Soc.,* To be published.
47. Petkov, V., Billinge, S. J. L., Vogt, T., Ichimura, A. S. & Dye, J. L., 2002, *Phys. Rev. Lett.,* **89,** 075502.
48. Billinge, S. J. L., McKimmey, E. J., Shatnawi, M., Kim, H., Petkov, V., Wermeille, D. & Pinnavaia, T. J., 2005, *J. Am. Chem. Soc*., **127,** 8492—8498.
49. Shatnawi, M., Paglia, G., Dye, J. L., Cram, K. D., Lefenfeld, M. & Billinge, S. J. L., 2007, *J. Am. Chem. Soc.,* **129,** 1386—1392.
50. Chupas, P. J., Qiu, X., Hanson, J. C., Lee, P. L., Grey, C. P. & Billinge, S. J. L., 2003, *J. Appl. Crystallogr.,* **36,** 1342—1347.

Acknowledgements. I would like to acknowledge the hard work and dedication of all Billinge-group members, past and present, who have done so much to further the PDF technique in the group. Also, all the help, support and x-rays and neutrons that we have received from national user facilities that made our work possible. Finally I would like to acknowledge funding from NSF, the most recent grant being DMR-0304391, and DOE through grant DE FG02 97ER45651.